CHAPTER 2

HYDROTHERMAL CRYSTAL GROWTH, STRUCTURES AND THERMAL PROPERTIES OF Co(II)-4,4′-BIPYRIDINE BASED COORDINATION POLYMERIC MATERIALS

2.1 Introduction

Among various materials playing an important role in modern materials research, inorganic-organic hybrid frameworks or so-called coordination polymeric materials have attracted worldwide attentions [97-99]. The prime motivations are due to inherent potentials for various applications, *e.g.* catalysis, separation, gas storage, sensing, ion exchange and magnetism with superiority over other corresponding conventional materials [100-104]. The strategies adopted in the preparation of these polymeric materials have mostly been based on conventional solution technique using organic solvents, until a technique namely "hydrothermal synthesis" has been introduced [105]. The technique has proved to be an effective approach in the preparation and crystal growth of many important solids, *e.g.* microporous crystals, complex oxide ceramics and magnetic materials [82, 106]. The fast kinetics of nucleation and crystal growth under hydrothermal conditions, however, generally lead to crystals of poor quality. This then hinders the achievement of structural knowledge, particularly of new materials, due to the fact that the structures of these generally insoluble polymeric materials can so far only be determined by single crystal X-ray

diffraction technique. The disadvantages hence hamper the success in using hydrothermal synthesis in preparing new coordination polymeric materials with full understanding of their structures [107]. Thermodynamic and kinetic parameters under hydrothermal conditions however can be subtly manipulated, in the cases where their influences on the formation and crystal growth of the desired phase are known.

The present work reports the attempts to optimize these hydrothermal parameters in order to prepare single crystals of new Co(II)-4,4′-bipyridine based coordination polymeric materials with suitable quality for structural characterization. The influences of these parameters on phase formation and crystal growth are investigated for relative structural design. The crystal structures of two coordination polymeric materials, one of which has been revealed to be a new compound with complicated and unique structure, and thermal behavior are reported.

2.2 Experimental

2.2.1 Hydrothermal Single Crystal Growth

The reaction mixtures were prepared from cobalt (II) nitrate hexahydrate ($Co(NO_3)_2.6H_2O$, 98% Aldrich), 4,4′-bipyridine (4,4′-bipy, $C_{10}H_8N_2$, 99% Fluka) and sulfuric acid (H_2SO_4, 97% Aldrich) in deionized water. Some conditions of the hydrothermal reactions and physical appearance of obtained products are shown in Table A1 (Appendix A). The pH of the mixtures were adjusted using potassium hydroxide pellets (KOH, 98% Aldrich) to vary from 5.0 to 10.4. This led to the final molar ranges of $Co(NO_3)_2.6H_2O$/4,4′-bipy/H_2SO_4/KOH/H_2O to be 1/0.75-1.5/0.5-

2.5/1.0-6.6/100-560. Each mixture was stirred for 30 minutes, and sealed in a static hydrothermal reactor fitted with Teflon liner to 70% filling capacity. The reactions were carried out under autogeneous pressure at 150 and 180 ^{o}C for varied duration ranging from 6 to 72 h. The mixtures were then cooled down to room temperature with either slow cooling rate of 0.1 ^{o}C·min^{-1}, or rapid rate of 5.0 ^{o}C·min^{-1}. The solid products were recovered by filtration, and washed with deionized water before being left to dry in air.

2.2.2 Structural Characterization

Phase formation, purity and crystallinity of the bulk solids were characterized by powder X-ray diffraction (PXRD, Bruker D8 Advance, CuK_{α}, Ni Filter, λ=1.540558 Å, 48 kV, 30 mA). The presence of the organic motifs in the crystals was confirmed by CHNS/O analyzer (Perkin Elmer Series II 2400), and Fourier Transform Infrared spectroscopy (FT-IR, Bruker Tensor 27, 4000-400 cm^{-1}, resolution 0.5 cm^{-1}) using KBr discs.

Suitable crystals were chosen from bulk solids for further structural characterization by single crystal X-ray diffraction. Three distinct structures could be identified, including two coordination polymeric compounds; $[Co_2(H_2O)_2(OH)_2(4,4'\text{-bipy})_8](NO_3)_2.2(4,4'\text{-bipy}).10(H_2O)$ (**1**) and $[Co(SO_4)(H_2O)_3(4,4'\text{-bipy})].2(H_2O)$ (**2**). The other crystal was revealed to be a simple ionic framework of $K_4[Co(H_2O)_6]_2(SO_4)_4$ (**3**). The structures of **2** and **3** were formerly reported, although different preparative techniques were used to prepare single crystals [32, 108]. The structure of **1**, on the other hand, has not yet been reported before.

Reflection data of the chosen crystals of compounds **1**, **2** and **3** were collected on a Bruker SMART APEX CCD diffractometer at 298(2) K using graphite monochromated MoK_α radiation (λ=0.71073 Å). The collected data were reduced by the SAINT program [109] and empirical absorption correction was done by using the SADABS program [110]. The structures were solved and refined by direct method and successive different Fourier maps using SHELXS-97 [111] and SHELXL-97 [112] *via* the WinGX [113] interface. All of non-hydrogen atoms were located from direct and different Fourier maps and refined anisotropically. The hydrogen atoms were located geometrically and refined using a riding model provided in the SHELXL-97 program, in the cases where the attached atoms were ordered. The structures of **1** and **2** showed very high degree of disordering. No hydrogen atoms were therefore assigned to the disordered atoms, and many restraints were applied during the refinements. Table 2.1 contains crystals data, collection parameters, and refinement criteria for **1**, **2** and **3**.

2.2.3 Thermogravimetric Investigation of 1

Thermal behavior of **1** was studied on thermogravimetric analyzer (Perkin Elmer TGA7) using ground crystals. The measurements were conducted under nitrogen gas flow in a temperature range 50-600 ^oC with a heating rate of 20 $^oC \cdot min^{-1}$.

2.3 RESULTS AND DISCUSSION

2.3.1 Hydrothermal Single Crystal Growth

Among the investigated hydrothermal parameters, chemical composition

Table 2.1 Crystallographic data of $[Co_2(H_2O)_2(OH)_2(4,4'\text{-bipy})_8](NO_3)_2 \cdot 2(4,4'\text{-bipy}) \cdot 10(H_2O)$ (**1**), $[Co(SO_4)(H_2O)_3(4,4'\text{-bipy})] \cdot 2(H_2O)$ (**2**), and $K_2Co(H_2O)_6(SO_4)_2$ (**3**).

	1	**2**	**3**
CCDC no.	CCDC-618870	CCDC-618871	-
Formula	$Co_2N_{22}O_{20.335}C_{100}H_{94}$	$CoSN_2O_9C_{10}H_{18}$	$CoS_2K_2O_{14}H_{12}$
Formula weight	2041.83	401.25	437.35
Crystal size/mm^3	0.325x0.265x0.235	0.243x0.140x0.097	0.358x0.348x0.184
Crystal system	Orthorhombic	Trigonal	Monoclinic
Space group	*C2*	$P6_5$	$P2_1/c$
a/ Å	17.9884(14)	11.4288(8)	6.1704(9)
b/ Å	11.4661(9)	11.4288(8)	12.2703(18)
c/ Å	24.5480(12)	20.8978(15)	9.0943(14)
α/°	90	90	90
β/°	90	90	105.253(2)
γ/°	90	120	90
V_{cell}/Å^3	5063.2(6)	2363.9(3)	664.30(17)
Z	2	6	2
ρ_{calc}/g.cm^{-3}	1.339	1.691	2.186
T/K	298(2)	298(2)	298(2)
Radiation (λ/Å)	MoK_α (0.71073)	MoK_α (0.71073)	MoK_α (0.71073)
μ/mm^{-1}	0.407	1.269	2.299
θ_{min}, θ_{max}	1.66, 29.06	2.06, 28.28	2.85, 28.28
Total data	11222	3536	1585
Unique data	8865	3290	1553
Parameters no.	534	220	113
Restraints no.	51	21	1
Goodness of fit	1.058	1.018	1.100
R, R_w (all data)	0.0935, 0.2261	0.0416, 0.0815	0.0358, 0.1133
R, R_w($I>2\sigma(I)$)	0.0760, 0.2104	0.0377, 0.0800	0.0354, 0.1131

and pH of the reaction mixtures showed close correlation and significant influences on the formation of crystals as a pure and exclusive phase. The red crystals of **2** could be obtained as the only exclusive solid just when the molar ratio of $Co(NO_3)_2.6H_2O$/ 4,4′-bipy/H_2O and the pH of the reaction mixture were adjusted to be precisely 1.0/0.75/150 and 7.0 respectively. The PXRD pattern of the bulk crystals compared with simulated pattern calculated from the crystal data of **2** is shown in Figure 2.1.

The two patterns are alike, suggesting the crystal to be a genuine representative of the bulk solid. Slight deviation of the reaction pH resulted in the formation of the ionic framework **3**, either as a mixture or pure phase. The orange crystals of **1**, in contrary to **2**, could not be obtained as the only phase in any case. It was always present as a mixture with other phases, particularly of **2**, implying the preferable formation of **2**. The excess amount of 4,4′-bipy and alkali environment apparently favored the crystal growth of **1**. The $Co(NO_3)_2.6H_2O$/4,4′-bipy mole ratio of 1/1.5 and a wide pH range of $7.7 \leq pH \leq 10.4$ provided crystals of **1** with suitable quality for further structural characterization. The alkali environment apparently provided a large amount of hydroxyl groups, which then coordinate to the framework Co(II) centers as revealed later by single crystal X-ray diffraction experiment. The absence of sulfate groups in the framework of **1** also indicated the outnumbering of the hydroxyl groups compared to the bulkier sulfate at alkali pH region, used in the preparation of **1**. This then accounted for the coordination of the hydroxyl ligands to the framework Co(II) centers, rather than the sulfate groups. At the neutral pH used in the preparation of **2**, this would not be the case resulting in the present of the sulfate and the absence of the hydroxyl ligands. The necessity for an excess amount of 4,4′-bipy in the reaction mixture was also prominent for the growth of **1**. The Co(II): 4,4′-bipy in the chemical formula of **1**, obtained from single crystal experiment, is as high as 1:10, compared to 1:1 in the case of **2**.

In contrast to chemical composition and pH of the reaction mixtures, the reaction temperature, time and rate of cooling were not as crucial.

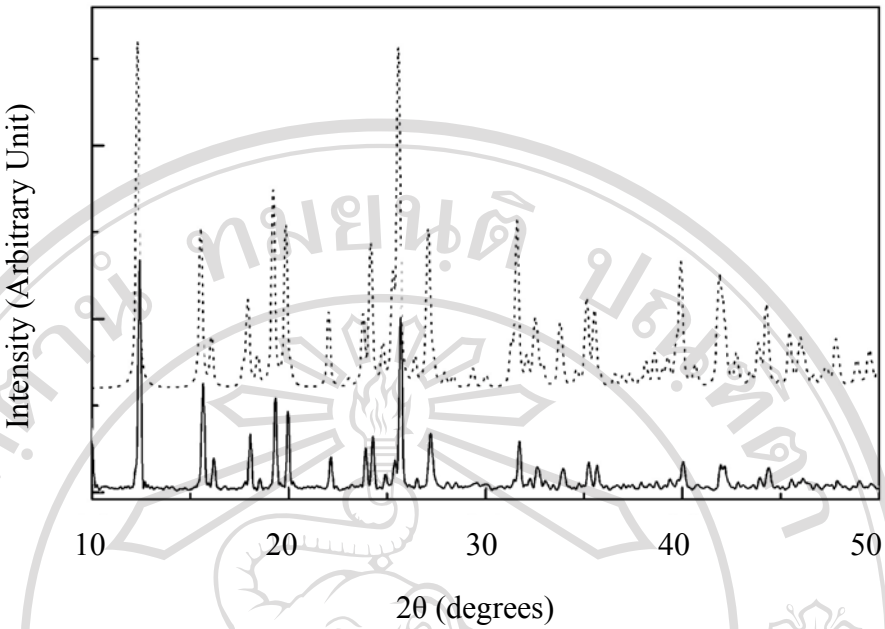

Figure 2.1 PXRD pattern taken from ground crystals (solid line) of **2** compared with simulated pattern (dotted line) calculated from the single crystal data

2.3.2 Crystal Structures of 2 and 3

The crystal structure of **2** obtained from the hydrothermal reactions as-described is well consistent with the structure reported by J. Lu, C. Yu, T. Niu, T. Paliwala, G. Crisci, F. Somosa and A.J. Jacobson [32], and therefore will not be described in detail. Few intriguing notions, however, can be addressed. The atomic coordination environment present in **2** is shown in Figure 2.2(a) with 50% thermal ellipsoids. The refined atomic coordinates and equivalent isotropic thermal parameters are shown in Table 2.2. Selected bond distances and angles are summarized in Table 2.3. The disordering of *ca.* 50% between two sties for each C atoms in one of the phenyl ring of the bridging 4,4′-bipy is apparent. This can be accounted for by the disordering dispensation from the water located in vicinity. The coplanarity of the two

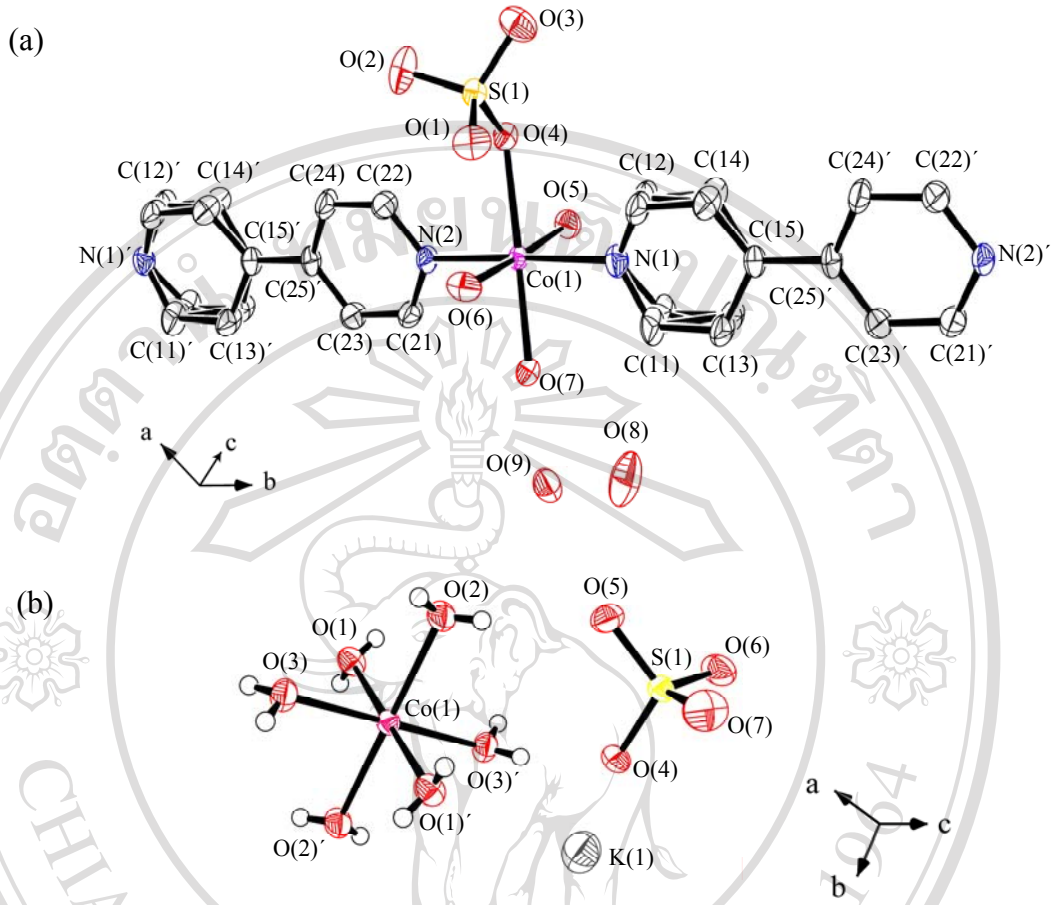

Figure 2.2 View of the extended asymmetric unit of (a) **2** and (b) **3** showing atomic coordination environments and 50% thermal ellipsoids, with atomic numbering schemes.

phenyl rings can roughly be approximated. The Co(II) atom adopts nearly regular octahedral environment coordinating to four O atoms, three of which are of water and the other of the sulfate pendant, and two crystallographically distinct N atoms from two *trans* 4,4′-bipy molecules. The 4,4′-bipy molecules in **2** play a crucial role in linking two adjacent Co(II) atoms to form one-dimensional chains aligning along the *a* and *b* axes in the *ab* plane. The refined Co(II)-O bond distances (Table 2.3) are well agreed with the earlier report, although that of Co(II)-O(SO_3) is significantly longer than the

Table 2.2 Refined atomic positions ($x10^{-4}$) and relevant equivalent isotropic thermal parameters ($Å^2 \times 10^{-4}$) of atoms in the asymmetric units of **2**

Atom	x	y	z	Ueq
Co(1)	-1(4)	4322.2(4)	311.90(19)	186.8(10)
S(1)	3436.7(8)	6109.6(8)	51.9(4)	229.6(17)
N(1)	-35(3)	6206(3)	284.3(16)	297(6)
N(2)	-0.0070(3)	2400(3)	356.3(14)	234(5)
O(1)	3008(3)	6346(3)	-574.2(11)	357(6)
O(2)	3979(3)	5194(3)	-26.9(14)	453(7)
O(3)	4458(3)	7394(3)	327.0(14)	411(6)
O(4)	2238(2)	5460(2)	493.7(10)	240(5)
O(5)	-248(3)	4286(3)	1297.7(13)	312(6)
O(6)	375(3)	4415(3)	-645.4(12)	327(6)
O(7)	-2132(2)	3211(2)	117.9(11)	263(5)
O(8)	-4678(4)	3751(4)	-315.5(17)	657(10)
O(9)	-5619(3)	1157(3)	204.5(14)	447(7)
C(11A)	-1168(12)	6230(14)	132(5)	370(20)
C(11B)	-1196(12)	6222(14)	407(5)	370(20)
C(12A)	1070(17)	7405(15)	196(6)	340(30)
C(12B)	1069(17)	7355(15)	428(6)	340(30)
C(13A)	-1250(20)	7417(17)	159(6)	370(30)
C(13B)	-1230(20)	7432(17)	418(6)	370(30)
C(14A)	1135(11)	8662(14)	209(4)	279(18)
C(14B)	1070(11)	8562(14)	461(4)	279(18)
C(15)	-74(3)	8641(3)	322(2)	244(6)
C(21)	-1224(4)	1214(3)	369(2)	318(7)
C(22)	1068(4)	2349(3)	340(2)	316(7)
C(23)	-1270(4)	-23(3)	354(2)	313(7)
C(24)	1107(4)	1158(3)	332(2)	320(8)
C(25)	-81(4)	-59(3)	337.9(19)	245(6)

Table 2.3 Selected bond distances and angles for **2**.

Bond distances (Å)			
Co(1)-O(4)	*2.247(2)*	S(1)-O(1)	1.469(2)
Co(1)-O(5)	*2.077(3)*	S(1)-O(2)	1.468(3)
Co(1)-O(6)	*2.038(3)*	S(1)-O(3)	1.461(3)
Co(1)-O(7)	2.150(2)	*S(1)-O(4)*	*1.505(2)*
Co(1)-N(1)	2.175(3)		
Co(1)-N(2)	2.160(2)		
Bond angles (°)			
O(5)-Co(1)-O(4)	87.04(9)	O(5)-Co(1)-N(2)	90.11(11)
O(5)-Co(1)-O(7)	94.14(10)	O(6)-Co(1)-N(2)	89.70(11)
O(6)-Co(1)-O(4)	89.24(10)	O(7)-Co(1)-N(2)	87.28(9)
O(6)-Co(1)-O(7)	89.58(10)	O(1)-S(1)-O(2)	109.25(17)
O(4)-Co(1)-N(1)	90.63(10)	O(1)-S(1)-O(3)	109.75(17)
O(5)-Co(1)-N(1)	88.63(11)	O(1)-S(1)-O(4)	109.41(14)
O(6)-Co(1)-N(1)	91.73(12)	O(2)-S(1)-O(3)	110.53(18)
O(7)-Co(1)-N(1)	90.20(10)	O(2)-S(1)-O(4)	108.76(15)
O(4)-Co(1)-N(2)	91.92(9)	O(3)-S(1)-O(4)	109.12(16)

others due to the Jahn-Teller effect. This results in two substantially shorter Co(II)-OH_2 bonds located in the *cis* position relative to the Co(II)-O(SO_3) bond, and a long coordinating S-O bond compared to the terminal S-O bonds of the sulfate pendant. These bonds are shown in italic in Table 2.3. The bond elongation between the C atoms bridging two phenyl rings of the same 4,4′-bipy molecule (C(15)-C(25), 1.491(4) Å), in comparison to those within the ring (1.36(2)-1.41(2) Å), may also be noted.

The crystal structure of the ionic framework **3**, with asymmetric unit shown in Figure 2.2(b), was well documented by A. Kirfel, H. Klapper, W. Schafer and F. Schwabenlander, although different cell setting was chosen; $P2_1/a$, a=9.057(1) Å,

b=12.211(2) Å, *c*=6.155(1) Å, *β*=104.82(1)°, Z=2, R=0.0188, R_w=0.0504, S=1.14 [14]. The refined atomic coordinates and equivalent isotropic thermal parameters are shown in Table 2.4. The refined bond distances and angles for **3** are shown in Table 2.5.

Table 2.4 Refined atomic positions ($x10^{-4}$) and relevant equivalent isotropic thermal parameters ($Å^2 \times 10^{-3}$) of atoms in the asymmetric units of **3**

Atom	x	y	z	Ueq
Co(1)	5000	5000	5000	182(2)
K(1)	1572.6(14)	6528.5(7)	8675.8(10)	427(3)
S(1)	2279.3(11)	3643.8(5)	9104.1(7)	215(2)
O(1)	5341(4)	3862(2)	3314(3)	263(5)
O(2)	3345(4)	6114.2(19)	3301(3)	277(5)
O(3)	8007(4)	5685(2)	4971(3)	268(5)
O(4)	1192(4)	4376.0(17)	7833(2)	273(5)
O(5)	4468(4)	32597(18)	8918(3)	313(5)
O(6)	777(4)	27061(19)	9090(3)	382(6)
O(7)	2595(5)	4243(2)	10534(3)	458(7)

Table 2.5 Selected bond distances and angles for **3**.

Bond distances (Å)			
Co(1)-O(1)	2.125(2)	S(1)-O(4)	1.478(2)
Co(1)-O(2)	2.114(2)	S(1)-O(5)	1.482(2)
Co(1)-O(3)	2.044(2)	S(1)-O(6)	1.475(2)
		S(1)-O(7)	1.461(2)
Bond angles (°)			
O(1)-Co(1)-O(2)	91.04(10)	O(4)-S(1)-O(5)	110.10(13)
O(1)-Co(1)-O(3)	89.89(10)	O(4)-S(1)-O(6)	108.20(14)
O(2)-Co(1)-O(3)	89.43(9)	O(4)-S(1)-O(7)	108.48(14)
		O(5)-S(1)-O(6)	109.90(14)
		O(5)-S(1)-O(7)	110.46(16)
		O(6)-S(1)-O(7)	109.66(17)

2.3.3 Crystal Structure of 1

The crystal structure of **1** was particularly unwieldy due to a large number of non-hydrogen atoms present in the asymmetric unit, and high degree of disordering as shown in Figure 2.3(a) and Figure 2.3(b). In order to successfully solve and refine the structure, the racemic twin law with two twin components was necessarily applied, leading to a large number of restraints and constrains (Table 2.1). The refined atomic coordinates and equivalent isotropic thermal parameters are shown in Table 2.6. The refined bond distances and angles are summarized in Table 2.7, and well consistent with the other related structures [32, 52]. There are two crystallographically distinct Co(II) atoms, *i.e.* Co(1) and Co(2), residing in the special positions, and therefore were refined with positional constraints. Figure 2.3(a) shows the extended framework of **1**, exhibiting an octahedral environment of the Co(II) atoms. Each Co(II) atom coordinates to four N atoms, including two atoms from two *trans* terminal 4,4′-bipy, and the other two from two *trans* bridging 4,4′-bipy. The Co(II)-4,4′-bipy-Co(II) linkages lead to a formation of a one-dimensional chain substructure, which can be described in crystal engineering terms as being constructed from Co(II) nodes and 4,4′-bipy node linkers. The Co(1) octahedral sphere is completed by two *trans* hydroxyl groups, neutralizing the positive charges on the metal. This results in a neutral $[Co(1)(OH)_2(4,4'\text{-bipy})_4]$ chain, assigned as chain **A** hereafter. The coordination environment of Co(2) is closely similar to that of Co(1), with the only difference in the fulfillment of the octahedral sphere with two *trans* aqua ligands in stead of the hydroxyl groups. The positively charged $[Co(H_2O)_2(4,4'\text{-bipy})_4]^{2+}$ one-dimensional chain substructure, assigned as chain **B**, is therefore

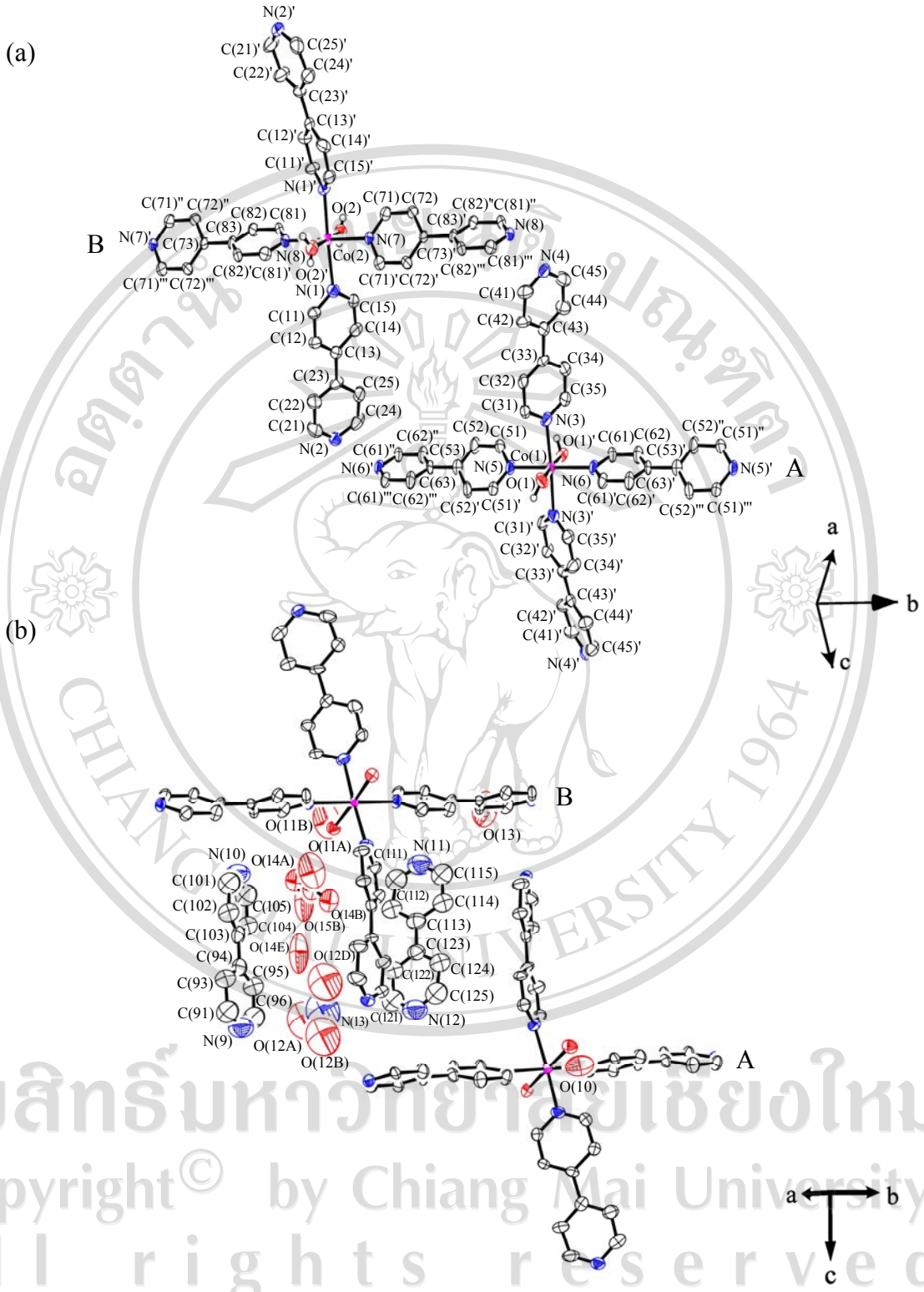

Figure 2.3 View of (a) the partial framework of **1** revealing two distinct octahedral Co(II), and the one-dimensional **A** and **B** substructural units, and (b) the occluded guest species with 50% thermal ellipsoids. Hydrogen atoms of 4,4′-bipy molecules and water of crystallization are omitted for clarity.

Table 2.6 Refined atomic positions ($x10^{-4}$) and relevant equivalent isotropic thermal parameters ($Å^2 \times 10^{-3}$) of atoms in the asymmetric units of **1**.

Atom	x	y	z	U_{eq}
Co(1)	5000	8543.3(10)	5000	29.6(4)
Co(2)	5000	526.1(9)	0	26.2(4)
O(1)	3935(4)	8598(7)	4609(2)	42.3(15)
O(2)	6046(3)	475(7)	398(2)	37.9(14)
O(10)	2647(6)	7694(13)	4949(4)	104(4)
O(11A)	8195(18)	1190(40)	1070(20)	173(11)
O(11B)	7370(10)	1290(30)	0.0178(13)	173(11)
O(12A)	8556(16)	760(30)	3858(12)	247(7)
O(12B)	7583(15)	760(30)	4175(12)	247(7)
O(12D)	7722(15)	1110(20)	3166(13)	247(7)
O(13)	7508(8)	8760(20)	5(9)	200(9)
O(14A)	9130(18)	1170(30)	1200(16)	84(5)
O(14B)	8103(13)	1810(20)	1645(11)	84(5)
O(14E)	8622(17)	1510(20)	1395(11)	84(5)
O(15A)	8998(12)	1050(20)	2582(16)	178(12)
O(15B)	9118(18)	1520(30)	1610(20)	178(12)
C(11)	3991(5)	-129(9)	947(3)	39(2)
C(12)	3810(5)	-277(9)	1477(3)	36(2)
C(13)	4162(5)	309(8)	1901(3)	32(2)
C(14)	4705(6)	1083(10)	1741(4)	44(2)
C(15)	4878(6)	1156(9)	1212(4)	40(2)
C(21)	3511(7)	-1038(11)	3187(4)	59(3)
C(22)	3606(7)	-817(11)	2628(4)	53(3)
C(23)	4018(6)	104(9)	2484(3)	38(2)
C(24)	4311(6)	827(9)	2903(4)	45(2)
C(25)	4182(6)	551(11)	3434(4)	52(2)
C(31)	5126(5)	7772(8)	3803(4)	37(2)
C(32)	5288(5)	7846(8)	3254(3)	35(2)
C(33)	5770(5)	8660(10)	3090(3)	34.4(19)
C(34)	6134(7)	9385(10)	3488(4)	51(3)
C(35)	5945(5)	9254(9)	4029(4)	40(2)
C(41)	5663(6)	8471(12)	1547(4)	50(3)
C(42)	5528(6)	8227(10)	2092(3)	46(3)
C(43)	5938(5)	8840(8)	2504(4)	34(2)
C(44)	6461(6)	9628(11)	2335(4)	49(2)
C(45)	6554(6)	9772(11)	1792(4)	53(3)
C(51)	5608(6)	6044(9)	4902(4)	38(2)
C(52)	5635(7)	4855(9)	4893(4)	44(3)
C(53)	5000	4218(12)	5000	33(3)
C(61)	4361(6)	11109(8)	4886(3)	34(2)
C(62)	4360(7)	12294(9)	4885(4)	45(3)

Table 2.6 Refined atomic positions ($x10^{-4}$) and relevant equivalent isotropic thermal parameters ($Å^2 \times 10^{-3}$) of atoms in the asymmetric units of **1** (Continue)

Atom	x	y	z	U_{eq}
C(63)	5000	2925(12)	5000	42(4)
C(71)	5567(6)	3005(9)	-191(3)	40(2)
C(72)	5581(5)	4212(8)	-195(3)	35(2)
C(73)	5000	-5169(11)	0	37(4)
C(81)	5612(5)	-2012(8)	81(4)	36(2)
C(82)	5654(5)	-3246(8)	92(3)	30.8(19)
C(83)	5000	-3878(11)	0	27(3)
C(91)	7154(10)	-3678(18)	3626(7)	111(2)
C(92)	7210(9)	-3651(15)	3026(6)	90.2(15)
C(93)	7624(7)	-2695(12)	2818(5)	70(3)
C(94)	7898(9)	-1935(15)	3188(6)	90.2(15)
C(95)	7799(11)	-2060(20)	3755(7)	111(2)
C(101)	7490(10)	-3045(17)	1295(7)	111(2)
C(102)	7350(9)	-3249(15)	1828(6)	90.2(15)
C(103)	7719(7)	-2602(11)	2225(5)	63(3)
C(104)	8229(10)	-1788(14)	2050(6)	90.2(15)
C(105)	8311(11)	-1703(18)	1491(7)	111(2)
C(111)	6643(10)	3659(17)	1356(7)	111(2)
C(112)	6523(9)	3276(14)	1895(6)	90.2(15)
C(113)	5970(7)	3849(11)	2148(4)	64(3)
C(114)	5552(9)	4729(14)	1852(6)	90.2(15)
C(115)	5754(11)	4950(18)	1319(7)	111(2)
C(121)	6014(10)	2647(17)	3593(7)	111(2)
C(122)	6193(9)	2875(15)	3034(6)	90.2(15)
C(123)	5779(7)	3606(10)	2724(4)	64(3)
C(124)	5177(9)	4093(14)	2945(6)	90.2(15)
C(125)	5064(11)	3754(18)	3507(7)	111(2)
N(1)	4542(4)	574(8)	804(3)	37.6(11)
N(2)	3788(4)	-399(7)	3575(3)	37.6(11)
N(3)	5442(4)	8498(8)	4185(3)	40.1(12)
N(4)	6148(4)	9212(6)	1388(3)	40.1(12)
N(5)	5000	6674(10)	5000	38(17)
N(6)	5000	10493(11)	5000	38.0(17)
N(7)	5000	2403(9)	0	29.3(14)
N(8)	5000	-1413(11)	0	29.3(14)
N(9)	7442(9)	-2925(16)	3927(6)	113(2)
N(10)	7950(9)	-2295(16)	1111(6)	113(2)
N(11)	6262(8)	4422(14)	1106(5)	113(2)
N(12)	5460(9)	3102(15)	3784(6)	113(2)
N(13)	7891(19)	1080(30)	3711(12)	247(7)

Table 2.7 Selected bond distances and angles for **1**

Bond distances (Å)			
Co(1)-O(1)	2.144(6)	N(13)-O(12A)	1.30(3)
Co(1)-N(3)	2.153(7)	N(13)-O(12B)	1.32(2)
Co(1)-N(5)	2.143(12)	N(13)-O(12D)	1.37(2)
Co(1)-N(6)	2.235(13)		
Co(2)-O(2)	2.121(6)		
Co(2)-N(1)	2.139(6)		
Co(2)-N(7)	2.152(11)		
Co(2)-N(8)	2.224(12)		
Bond angles (°)			
O(1)-Co(1)-N(3)	85.1(3)	O(2)-Co(2)-N(1)	85.3(2)
O(1)-Co(1)-N(5)	91.7(2)	O(2)-Co(2)-N(7)	91.6(2)
O(1)-Co(1)-N(6)	88.3(2)	O(2)-Co(2)-N(8)	88.4(2)
N(3)-Co(1)-N(5)	88.6(2)	N(1)-Co(2)-N(7)	88.5(3)
N(3)-Co(1)-N(6)	91.4(2)	N(1)-Co(2)-N(8)	91.5(3)
N(5)-Co(1)-N(6)	180.000(5)	N(7)-Co(2)-N(8)	180.0
		O(12A)-N(13)-O(12B)	94(3)
		O(12A)-N(13)-O(12D)	119(3)
		O(12B)-N(13)-O(12D)	139(3)

formed. The phenyl rings of the bridging 4,4′-bipy in both chains are puckered, whereas those of the terminal 4,4′-bipy are approximately coplanar. The novelty of the presence of both neutral and charged one-dimensional substructures sharing the common node and node linker in the same polymeric framework should be noted.

Chains **A** and **B** align along the common *b* axis, and are stacked by the space of *c*/2 unit along the *c* axis in a regular **ABAB** registry as shown in Figure 2.4(a). This leads to the formation of a two-dimensional layered structure in the *bc* plane. The interplay of hydrogen bonding and π-π interactions between the overlapping 4,4′-bipy terminal ligands of the two adjacent chains hold the chains

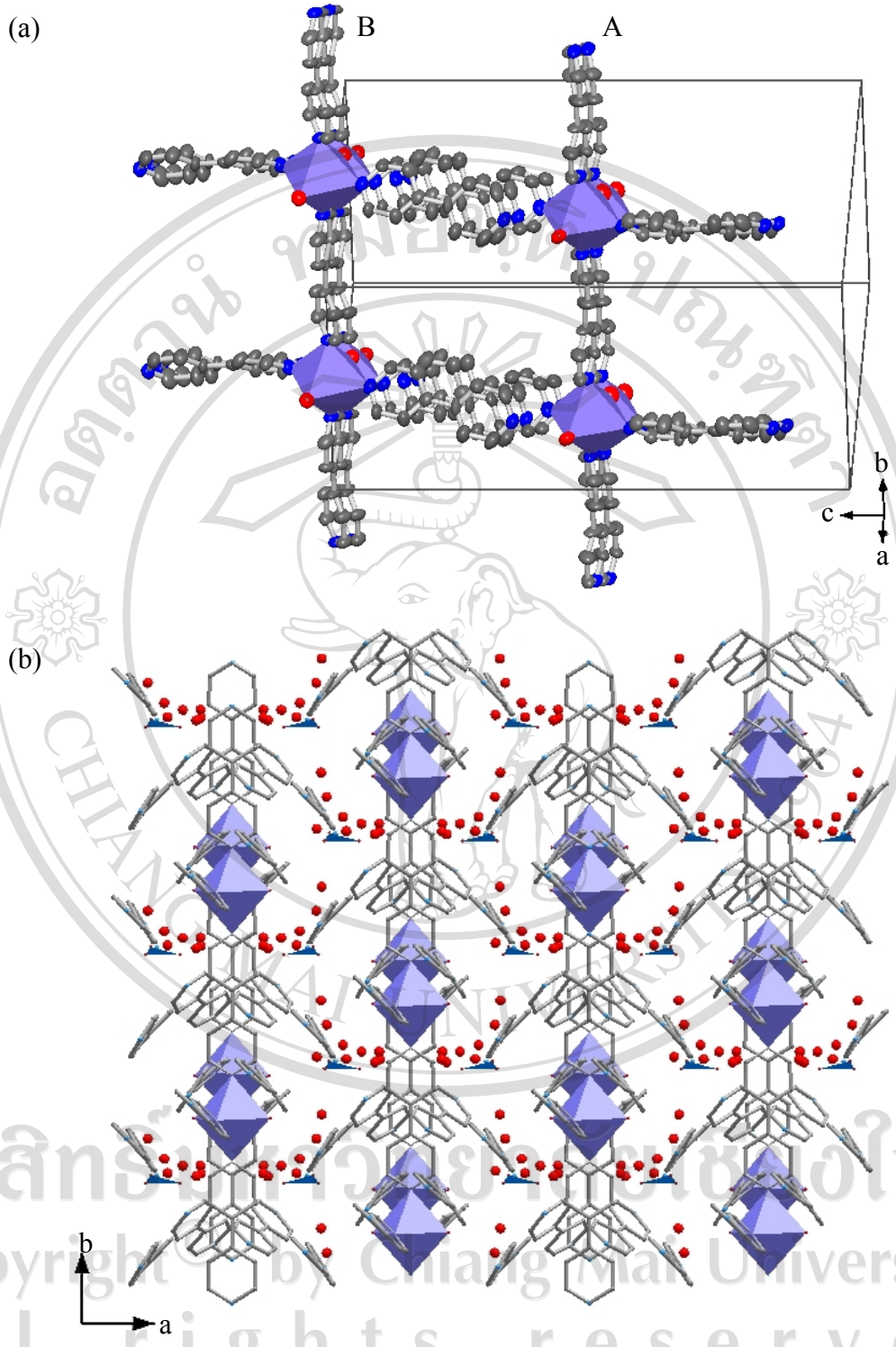

Figure 2.4 (a) The formation of **ABAB** layered structure in the *bc* plane with the rectangular cavities, and (b) the arrangement of the layers along the *a* axis to form three-dimensional framework with water, 4,4′-bipy and nitrate guest molecules in interlayered space.

together within the layers. The **ABAB** layers in the *bc* plane are packed along the *a* axis with a spacing of *a*/2 (Figure 2.4(b)) with the shortest interlayered distance of *ca.* 8 Å to complete the structure in the third dimension. The positively charged $[Co_2(H_2O)_2(OH)_2(4,4'\text{-bipy})_8]^{2+}$ three-dimensional framework is then constructed. The established polymeric framework bares structural resemblance to the frameworks found in $[Co(4,4'\text{-bipy})_3(H_2O)_2](ClO_4)_2 \cdot 1.4(4,4'\text{-bipy}) \cdot 3H_2O$ [52] and $[Ni(4,4'\text{-bipy})_{2.5}(H_2O)_2](ClO_4)_2 \cdot 1.5(4,4'\text{-bipy}) \cdot 2H_2O$ [114], although myriad structural aspects are prominently distinguished.

The adjacent **A** and **B** chains define partially hydrophilic-hydrophobic, rectangular cavities. Each cavity is enclosed by four Co(II) atoms at the corners and six 4,4′-bipy molecules, including one bridging 4,4′-bipy on edges along the chain and two each on edges between the chains (Figure 2.4(a)). The effective size of the cavities is *ca.* 8.0 x 10.0 $Å^2$. The cavities are filled with the 4,4′-bipy guest molecules, nitrate counter ions, and the water of crystallization as shown in Figure 2.4(b), leading to the complete crystal formula $[Co_2(H_2O)_2(OH)_2(4,4'\text{-bipy})_8](NO_3)_2 \cdot 2(4,4'\text{-bipy}) \cdot 10(H_2O)$. Two distinctive 4,4′-bipy guest molecules can be identified. These include the one oriented almost at right angle relative to the π-π interacting 4,4′-bipy ligands, and just inside the cavities. The other 4,4′-bipy guest molecules are located nearly parallel to the π-π interacting 4,4′-bipy ligands, just outside the cavities and in the interlayer gallery. The majority of the water guest molecules are highly disordered in the interlayer space, and the site summation restraints were applied during the refinement, providing a specific quantity of 10.33 molecules in the formula unit to give the best statistical values.

The FT-IR spectrum (Appendix B; Figure B1) was used to confirm the presence of the organic species. The spectral assignments are presented in Table 2.8. The strong and broad vibrational bands region (3500-3120 cm^{-1}) indicated OH stretching and hydrogen bonding of the water. The N-O stretching for nitrate counter ions can be identified from very strong vibrational bands at 1384 and 803 cm^{-1} [115].

Table 2.8 Spectral assignments for the FT-IR spectrum of **1**.

Wave number (cm-1)	Assignments
3500 - 3120 s,br	ν(O-H); water, H-bond
3083 s, 3046 s	ν(C-H); Aromatic
1600 vs, 1535 m, 1488 w	ν(C=C); Aromatic
1405 vs,	ν(C=N), δ(O-H)
1384 vs	ν(N-O)
1323 m	δ(C-H)
1221-1000 m-w, 818 vs	β(C-H); Aromatic
803 vs	γ(N-O)
624 s	ω(C-H); Aromatic

br = broad vs = very strong, s = strong, m = medium, w = weak,
ν = stretching, δ = bending, β = in-plane bending, γ = out-of-plane bending,
ω = wagging

2.3.4 Thermogravimetric Behavior of 1

Compound **1** was stable in air, showing alteration in neither color nor texture when it was left in ambient atmosphere. This was intriguingly contrary to the structural analogous $[Co(4,4'\text{-bipy})_3(H_2O)_2](ClO_4)_2 \cdot 1.4(4,4'\text{-bipy}) \cdot 3H_2O$ [52], which was allegedly unstable in air due to the loss of enclathrated guest molecules.

Thermogravimetric analysis of **1** showed complicated gradual weight losses pattern as shown in Figure 2.5. This corresponded well with the complicated structure involving several crystallographically different structural motifs. The initial gradual weight losses (14.5%) readily occurred at room temperature under the flow of nitrogen up to *ca.* 197 °C, and could be accounted for by the desolation of the surface water, and weakly bound water guest molecules (9.04%). The uncoordinated 4,4′-bipy guest molecules (calc. 15.21%, found 16.4%), followed by the counter ions (calc. 5.96%, found 6.3%) were assumingly removed in the temperature range 197-240 °C. According to the convoluted 4,4′-bipy ligands, a complicate pattern of approximately two major steps of weight losses was observed in the temperature range 240-360 °C, resulting in a black powder being amorphous to PXRD. This corresponded to eight equivalent 4,4′-bipy molecules in the chemical formula (calc. 60.85%, found 55.5%).

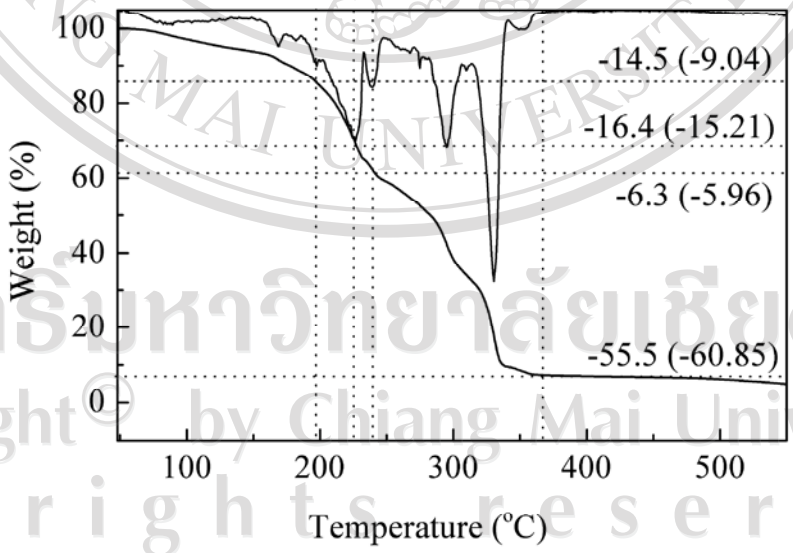

Figure 2.5 The TGA curve shows complicated weight losses on heating **1** under the $N_{2(g)}$ flow. The experimented figures are compared with the calculated figures present in the brackets.

2.4 Conclusions

Hydrothermal synthetic parameters were studied and optimized for the preparation of new coordination polymeric materials based on Co(II) and 4,4′-bipy. A new polymeric compound, $[Co_2(H_2O)_2(OH)_2(4,4'\text{-bipy})_8](NO_3)_2 \cdot 2(4,4'\text{-bipy}) \cdot 10(H_2O)$ **1** was prepared and structural characterized by single crystal experiment. The framework of **1** is made up of two different one-dimensional substructure, *i.e.* the neutral chain **A** and positively charged **B**, both of which sharing the same nodes and node linkers. This is rarely found, especially from one-pot crystal growth technique. Two other crystals are also identified, *i.e.* $[Co(SO_4)(H_2O)_3(4,4'\text{-bipy})] \cdot 2(H_2O)$, and $K_2Co(H_2O)_6(SO_4)_2$. The optimization of synthetic parameters apparently favors the formation of different polymeric structures, and this can be experimentally fine tuned. The information on influences of theses parameters can be employed with certain advantages in the future design of the relative structures.

2.5 Supplementary Materials

Crystallographic data (excluding structure factors) for the structures **1** and **2** have been deposited with the Cambridge Crystallographic Data Centre as supplementary publication no. CCDC-618870 and CCDC-618871. Copies of the data can be obtained free of charge on application to CCDC, 12 Union Road, Cambridge CB2 1EZ, UK (fax: (44) 1223 336-033; e-mail: deposit@ccdc. cam.ac.uk).